

Hyperbolic Pascal Simplex

László Németh*

(Communicated by Cihan Özgür)

ABSTRACT

In this article we introduce a new geometric object called hyperbolic Pascal simplex. This new object is presented by the regular hypercube mosaic in the 4-dimensional hyperbolic space. The definition of the hyperbolic Pascal simplex, whose hyperfaces are hyperbolic Pascal pyramids and whose faces are hyperbolic Pascals triangles, is a natural generalization of the definition of the hyperbolic Pascal triangle and pyramid. We describe the growing of the hyperbolic Pascal simplex considering the numbers and the values of the elements. Further figures illustrate the stepping from a level to the next one.

Keywords: Hyperbolic Pascal triangle; Pascal simplex; hypercube honeycomb; regular hypercube mosaic in 4-dimensional hyperbolic space, recurrence sequence.

AMS Subject Classification (2010): Primary: 05B45 ; Secondary: 52C22; 11B99.

1. Introduction

There are several generalizations of Pascal's arithmetical triangle (see, for instance [2, 3, 17]), there is among them the family of hyperbolic Pascal triangles. This new type is based on the hyperbolic regular mosaics denoted by Schläfli's symbol $\{p, q\}$, where $(p - 2)(q - 2) > 4$ (see [5]). Each regular mosaic induces a so-called hyperbolic Pascal triangle (HPT), it is detailed only for regular squared mosaics $\{4, q\}$ in [2, 9, 10, 11, 12]. Obviously, the classical Pascal's triangle is connected to the Euclidean square mosaic $\{4, 4\}$.

The 3-dimensional analogue of Pascal's original triangle is the well-known Pascal's pyramid (or more precisely Pascal's tetrahedron). Its levels are triangles and the numbers along the three edges of the n^{th} level are the numbers of the n^{th} lines of Pascal's triangle. Each number inside in any levels is the sum of the three adjacent numbers on the level above [1, 4, 8]. In [13] a 3-dimensional variation, the hyperbolic Pascal (cube) pyramid (HPP) is presented, which is based on the hyperbolic regular cube mosaic $\{4, 3, 5\}$. This object can also be considered as the a hyperbolic variation of the well-known (Euclidean) Pascal's pyramid which is built on the Euclidean regular cube mosaic $\{4, 3, 4\}$. In a special space, in $\mathbf{H}^2 \times \mathbf{R}$, there is an interesting generalization of HPP (see [15]).

In the 4-dimensional space the natural generalization of the square and the cube is the 4-dimensional hypercube. Coxeter [5] showed that the hypercube generates regular mosaics not only in the Euclidean, but also in the hyperbolic 4-dimensional spaces. They are the mosaics $\{4, 3, 3, 4\}$ and $\{4, 3, 3, 5\}$, respectively. The 4-dimensional Euclidean variation, Pascal's simplex can be based on the Euclidean hypercube mosaic $\{4, 3, 3, 4\}$.

In this article we present a 4-dimensional hyperbolic Pascal simplex (HPS) built on the mosaic $\{4, 3, 3, 5\}$. The method of the discussion is similar to the discussion of the hyperbolic Pascal pyramid's ([13]) case and we apply some of its results. (We keep the usual notation and write the hyperbolic Pascal simplex without an "apostrophe", similarly to the case of Pascal's classical triangle and the hyperbolic Pascal triangle.) We strictly follow the definitions and denotations of the hyperbolic Pascal triangle and pyramid in [2] and [13] (see also [15]). We mention that in the 4-dimensional Euclidean and hyperbolic spaces there are 2 and 4 other regular mosaics with bounded cells and vertex figures, but we do not examine them in this article. We suppose, that their examinations can be similar due to the generalization of Pascal triangle.

2. Construction of the hyperbolic Pascal simplex

The 4-dimensional hyperbolic hypercube mosaic $\{4, 3, 3, 5\}$ consists of hypercubes with Schläfli's symbol $\{4, 3, 3\}$. The vertex figures of the mosaic are 600-cells, $\{3, 3, 5\}$. The hypercube is well-known, but the 600-cell is not so much, thus we give some details of it. The cells of a 600-cell are tetrahedra ($\{3, 3\}$), the (2-dimensional) faces are triangles and the neighbouring vertices of a vertex of a 600-cell form an icosahedron ($\{3, 5\}$), so a vertex lies on 12 edges, 30 faces and 20 cells. Each edge is on 5 faces and 5 cells and each face connects 2 cells. The numbers of the vertices, edges, (2-dimensional) faces and cells of a 600-cell are 120, 720, 1200 and 600, respectively.

Considering an arbitrary vertex V of the mosaic, the number of hypercubes around V is 600, as many as the number of the cells of the 600-cell, and the number of the mosaic edges from V (degree of V) is 120, as many as the number of the vertices of the 600-cell. There are 20 hypercubes around a mosaic edge as there are 20 faces of an icosahedron, so there are 20 tetrahedra around a vertex on the 600-cell. See some other details of the hyperbolic hypercube mosaic in [5, 14, 16].

Let us consider an arbitrary vertex of the mosaic, say vertex V_0 , as the base vertex of \mathcal{HPS} . We sign it by 1 as well and let us sign all the vertices of the mosaic by the numbers of the shortest paths from the considered vertex to the base vertex along mosaic edges. The shortest paths imply a digraph directed from V_0 . We define a convex part \mathcal{P} of the mosaic the following way. First we take a hypercube with vertex V_0 and we consider the vertex V_1 opposite of V_0 in the hypercube. It is the furthest vertex of the hypercube from V_0 and it has the largest sign among the vertices, namely 24. Second we take the new hypercubes of the mosaic containing vertex V_1 and their vertices which have the largest signs in each hypercubes. Now we take again the hypercubes around these vertices and their vertices with the largest signs, and so on. Continuing this algorithm limitless, the set of these hypercubes gives \mathcal{P} . Finally, the vertices (labelled above) and the edges (directed above) of \mathcal{P} form an infinite digraph similar to an infinite simplex with a finite base vertex V_0 . We name it hyperbolic Pascal simplex (\mathcal{HPS}). Obviously, the signs of the vertices are the sums of the signs of the incoming edges.

Let level 0 be the vertex V_0 . Level n consists of the vertices of \mathcal{HPS} whose edge-distances from V_0 are n -edge (the distance of the shortest path along the edges of \mathcal{P} is n). The shapes of the levels are tetrahedra. It is clear, the 3-dimensional and 2-dimensional faces on the outer boundaries are hyperbolic Pascal pyramids and hyperbolic Pascal triangles based on mosaics $\{4, 5, 4\}$ and $\{4, 5\}$, respectively. The faces and edges of the n^{th} level are the n^{th} levels of \mathcal{HPP} and n^{th} lines of \mathcal{HPT} , respectively. Figures 1, 2 and 3 show the growing from a level to the next one in case of some lower levels. As each hyperface of \mathcal{HPS} is \mathcal{HPP} , there are six types of vertices: 1, A , B (from the 2-dimensional faces, which are hyperbolic Pascal triangles – see [2]) and C , D , E in the hyperfaces, corresponding to [13]. The properties of the growing come partly from the examination of \mathcal{HPT} and \mathcal{HPP} . We denote them, respectively, by grey, red, cyan, blue, green and yellow colours in the figures. The colours of the other different types of the vertices inside \mathcal{HPS} are also different. (See the definitions later. The first vertex inside of the simplex appears in level 4. It is the biggest, the purple sphere – vertex type F – in the centre of Figure 3.) The numbers without colouring refer to vertices in the lower level in every figure. The graphs, growing from a level to the new one, contain graph-cycles with six nodes. These graph-cycles figure the convex hulls of the parallel projections of the cubes from the mosaic, where the direction of the projection is not parallel to any edges of the cubes. Moreover, the rhombic-dodecahedra are the 3-dimensional shadows of the hypercubes.

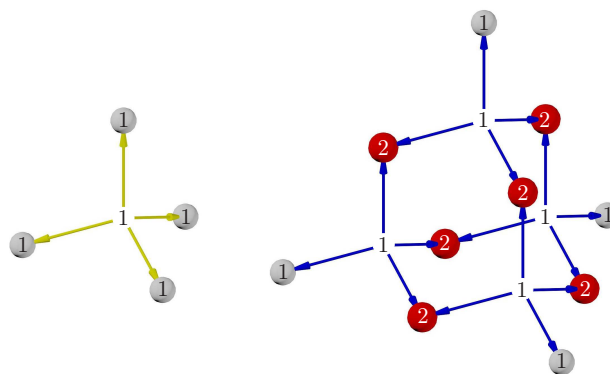


Figure 1. Connections between layers zero to one and one to two in \mathcal{HPS}

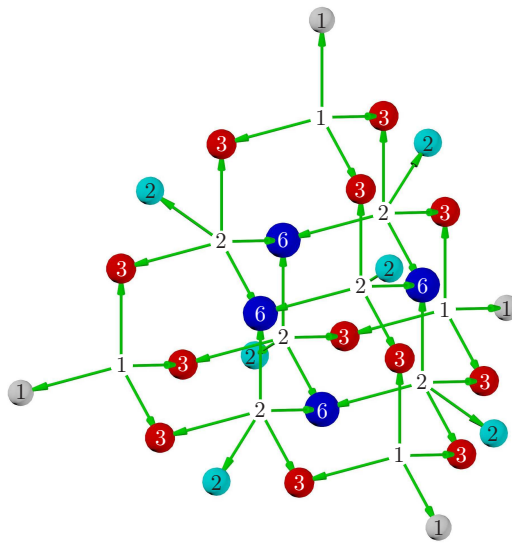


Figure 2. Connection between layers two and three in \mathcal{HPS}

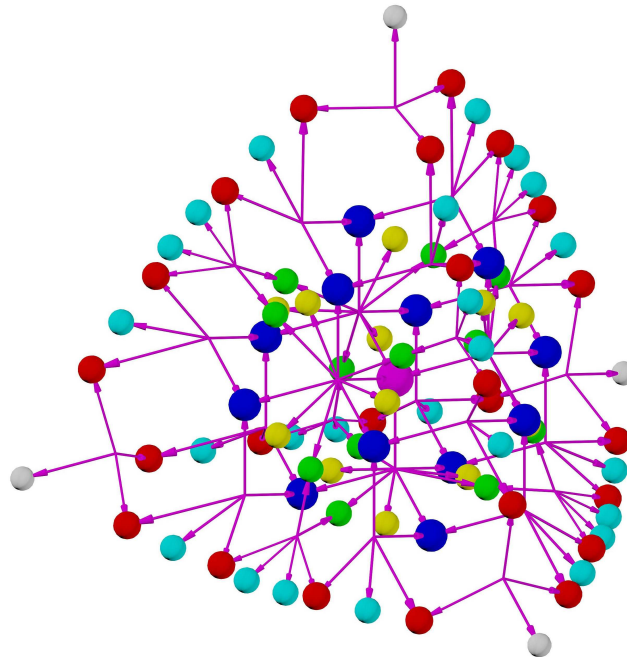


Figure 3. Connection between layers three and four in \mathcal{HPS}

In the following we describe the method of growing of the hyperbolic Pascal simplex and we give the sum of the paths connecting vertex V_0 to level n .

3. Growing of the hyperbolic Pascal simplex

In the classical Pascal's simplex the number of the elements on level n is $(n + 1)(n + 2)/2$ and its growing from level n to level $n + 1$ is $n + 2$. In this section we give the growing from level to level in the case of the hyperbolic Pascal simplex.

The growing process on the outer 2- and 3-dimensional faces of \mathcal{HPS} mostly comes from [13]. Figure 4 shows the growing of vertices types 1, A and B . For example, the centre figure illustrates that each vertex A has two incoming edges, which could be types 1, A or B , and five outgoing edges, precisely two A , one B and two C .

The degrees of 1, A and B are 5, 7 and 7, respectively.

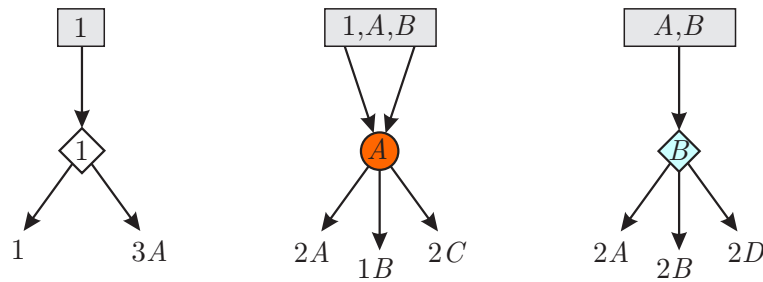


Figure 4. Growing of the 2-dimensional faces in \mathcal{HPS}

The vertices C , D and E are inside the 3-dimensional faces, which are \mathcal{HPP} -s and they have outgoing edges into the inside of \mathcal{HPS} . (There are 12 hypercubes around these edges in the mosaic.) Let us denote these new types of vertices by F , G and H (see Figure 5). So, the degrees of vertices C , D and E are 13. (Compare Figures 1–3 with Figures 4–5.)

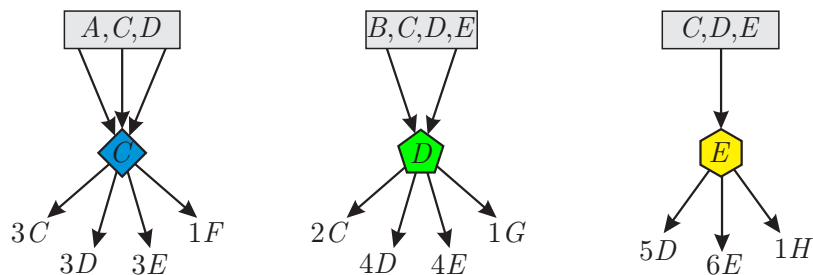


Figure 5. Growing of the 3-dimensional faces in \mathcal{HPS}

Now we examine the vertices inside \mathcal{HPS} . All these vertices have four, three, two or one incoming edges from the previous level. We denote them by types F , G , H and K , respectively. (In Figure 3 vertex F is coloured purple.) Some vertices F , G and H have one incoming edge from vertices C , D and E , respectively, and all vertices types F connect only to inside vertices of \mathcal{HPS} .

In the following we give the number of the outgoing edges of these vertices using the classification of the vertices of the vertex figures with a 4-dimensional generalized method applied in [13]. According to the previous section, the degrees of all these vertices are 120. Firstly, we consider a vertex type K in level i ($i \geq 5$). In the mosaic, the neighbouring vertices to K_i form a vertex figure, a 600-cell, whose all 120 vertices have mosaic edges joining to K_i . Among them there is only one vertex in level $i - 1$, we denote it by W_{i-1} (see Figure 6). The other vertices are in level $i + 1$ and with the classification of them we can give the numbers of different types of vertices which imply the outgoing mosaic edges from K_i . (The mosaic edge $W_{i-1}K_i$ is an incoming edge to K_i .) If a vertex of a 600-cell has one common edge with W_{i-1} , then it has two incoming mosaic edges. (We mention that the edges of the vertex figure are not the edges of the mosaic.) In Figure 6 vertex H_{i+1} connects to W_{i-1} , so there is a W_i mosaic vertex (not in the vertex figure) which has common mosaic edges not only with W_{i-1} but also with H_{i+1} . This way H_{i+1} has two incoming edges from W_i and K_i from level i , thus its type is H . All the vertices of the 600-cell which are adjacent to H_{i+1} form an icosahedron and the type of all its vertices are H (orange regular 9-gons in the figures). The type of the other 107 vertices of the 600-cell is K , as their incoming edges come from the considered vertex K_i .

Secondly, we take a vertex type H in level i ($i \geq 5$), let it be H_i in Figure 7. H_i has two incoming edges from level $i - 1$, so there are two vertices on the same edge of the vertex figure in level $i - 1$. We denote them by W_{i-1} again. (Generally, W denotes a vertex, whose type is not known or not important to know, while the index shows the level of the vertex.) Now we have to classify again the vertices of the vertex figure around the considered H_i according to its neighbouring vertices W_{i-1} . As there are 5 vertices in a 600-cell which are connected to both vertices by an edge, there are 5 vertices type G , they have 3 incoming edges from level i . (Recall, the mosaic edges and the icosahedron edges are different.) These 5 vertices are the intersections of the icosahedra connecting to the two W_{i-1} -s. In Figure 7 we drew the icosahedron connecting to the left vertex W_{i-1} and the vertices G_{i+1} are denoted by blue regular 8-gons. The other $2 \cdot 6$ vertices of the icosahedron are one-edge-long far from one of the W_{i-1} -s, so their types are H . The rest 101 vertices of the 600-cell are types K .

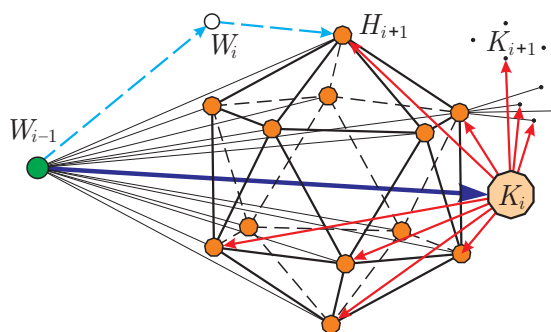


Figure 6. Growing method around vertex type K

On the right-hand side of the figure we highlighted the vertices W_{i-1} and G_{i+1} and their subgraph structure in the 600-cell.

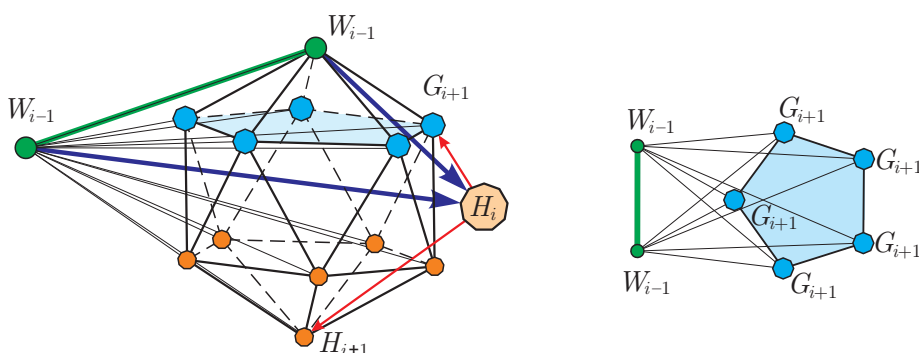


Figure 7. Growing method around vertex type H

Thirdly, we classify the vertices of the 600-cell in the case of a vertex G_i ($i \geq 5$). We mark a face of the 600-cell, its vertices are in level $i - 1$ and from them start the mosaic's incoming edges into G_i . There are only two vertices type F , which are neighbouring to all the three W_{i-1} -s. Thus both F_{i+1} have 4 incoming mosaic edges and Figure 8 shows them with yellow regular 7-gons. For all the three edges of triangle $W_{i-1}W_{i-1}W_{i-1}$ connect pentagons, so that the vertices are one-edge-long far from the endpoints of the edges. The type of their two common vertices are F , the other $3 \cdot 2$ vertices are G (see on the right-hand side in Figure 8). The other $3 \cdot 4$ vertices of the three icosahedra connecting to all W_{i-1} are H . The number of the rest vertices of the vertex figure is 97, their types are K .

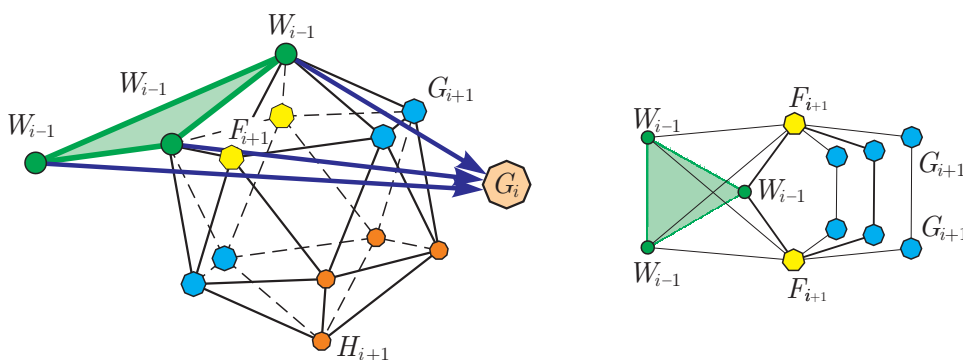


Figure 8. Growing method around vertex type G

Fourthly, we classify the vertices of the 600-cell in the case when the vertex is F_i ($i \geq 4$). Now a tetrahedron is in level $i - 1$ and from its vertices W_{i-1} start the incoming mosaic edges into the considered F_i . For all four faces of tetrahedron $W_{i-1}W_{i-1}W_{i-1}W_{i-1}$ connect a vertex F_{i+1} , so that they are joining to three W_{i-1} , so they have 4 incoming mosaic edges from level i (see Figure 9). That way along all the six edges of the tetrahedron there are 4 neighbouring vertices to the end of the edge. The rest, the fifth vertices are type G , the number of

them is $6 \cdot 1$. (There are 6 edges of a tetrahedron.) The other $4 \cdot 3$ vertices of the four icosahedra connecting to vertices W_{i-1} are type H . The rest vertices of the 600-cell are type K , they are 94 altogether.

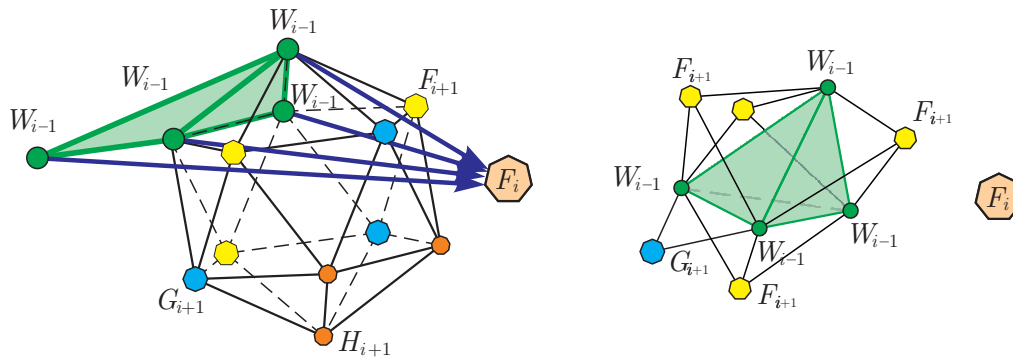


Figure 9. Growing method around vertex type F

Finally, in Figure 10 the growing method is presented in the case of the inner vertices of \mathcal{HPS} as a summing-up of discussions and figures. For example, the first graph shows that each vertex F has four incoming edges, which could be types C, F or G , and $120 - 4$ outgoing edges with 4 pieces F , 6 pieces of G , 12 pieces of H and 94 pieces of K .

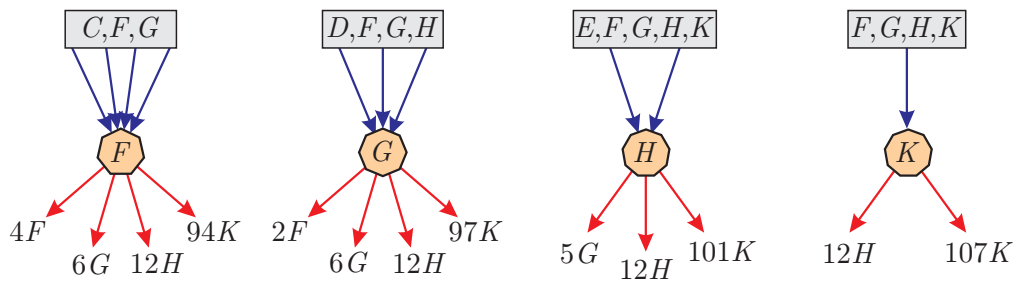


Figure 10. Growing inside \mathcal{HPS}

Figure 4, 5 and 10 describe the growing method of \mathcal{HPS} , but for summarising we have to consider the vertices in level $i + 1$ without multiplicity. For example the new vertices F are counted for all the vertices C, F and G . So, for the correct calculation we correspond only one third of them to the examined vertices C, F and G . Similarly for the cases of all vertices we eliminate the multiplicity.

Let us denote the sums of vertices types $A, B, C, D, E, F, G, H, K$ and 1 on level i by $a_i, b_i, c_i, d_i, e_i, f_i, g_i, h_i, k_i$ and v_i , respectively.

Summarising the details ($i \geq 4$) and calculating the numbers of vertices in some lower levels ($i < 4$) in Table 1, we proved the Theorem 3.1.

Theorem 3.1. *The growing of the numbers of the different types of vertices in \mathcal{HPS} is described by the system of linear homogeneous recurrence sequences ($n \geq 1$)*

$$\begin{aligned}
 a_{n+1} &= \frac{1}{2} (2a_n + 2b_n + 3v_n), \\
 b_{n+1} &= a_n + 2b_n, \\
 c_{n+1} &= \frac{1}{3} (2a_n + 3c_n + 2d_n), \\
 d_{n+1} &= \frac{1}{2} (2b_n + 3c_n + 4d_n + 5e_n), \\
 e_{n+1} &= 3c_n + 4d_n + 6e_n, \\
 f_{n+1} &= \frac{1}{4} (c_n + 4f_n + 2g_n), \\
 g_{n+1} &= \frac{1}{3} (d_n + 6f_n + 6g_n + 5h_n), \\
 h_{n+1} &= \frac{1}{2} (e_n + 12f_n + 12g_n + 12h_n + 12k_n), \\
 k_{n+1} &= 94f_n + 97g_n + 101h_n + 107k_n \\
 v_{n+1} &= v_n,
 \end{aligned} \tag{3.1}$$

with all zero and $v_1 = 4$ initial values.

Moreover, let s_n be the number of all the vertices in level n , so that $s_0 = 1$ and

$$s_n = a_n + b_n + c_n + d_n + e_n + f_n + g_n + h_n + k_n + 4, \quad (n \geq 1). \tag{3.2}$$

Table 1 shows the numbers of the different type of vertices on levels up to 10.

We show that our sequences are linear homogeneous recurrence sequences (with constant coefficients). For the definition and properties (and further references) of linear homogeneous recurrence sequences see [6].

Table 1. Number of types of the vertices $n \leq 10$

n	0	1	2	3	4	5	6	7	8	9	10
a_n	0	0	6	12	24	54	132	336	870	2268	5928
b_n	0	0	0	6	24	72	198	528	1392	3654	9576
c_n	0	0	0	4	12	36	136	696	4512	33004	253260
d_n	0	0	0	0	12	96	708	5388	41868	328116	2579232
e_n	0	0	0	0	12	156	1428	11808	9448	747936	5899092
f_n	0	0	0	0	1	4	16	86	1111	70970	7610192
g_n	0	0	0	0	0	6	72	1702	137462	15061942	1694955086
h_n	0	0	0	0	0	12	774	79254	8862504	998747934	112617248352
k_n	0	0	0	0	0	94	12228	1395058	157449038	17755598218	2002190230214
v_n	1	4	4	4	4	4	4	4	4	4	4
s_n	1	4	10	26	89	534	15696	1494860	166593249	18770594046	2116518790936

Theorem 3.2. *The sequences $\{a_n\}, \dots, \{k_n\}$ and $\{s_n\}$ can be described by the same ninth order linear homogeneous recurrence sequence*

$$\begin{aligned}
 x_n &= 128x_{n-1} - 1795x_{n-2} + 8837x_{n-3} - 19239x_{n-4} + 19239x_{n-5} \\
 &\quad - 8837x_{n-6} + 1795x_{n-7} - 128x_{n-8} + x_{n-9}, \quad (n \geq 10), \tag{3.3}
 \end{aligned}$$

the initial values are in Table 1. The sequences $\{a_n\}, \dots, \{e_n\}$ can also be described by

$$x_n = 12x_{n-1} - 37x_{n-2} + 37x_{n-3} - 12x_{n-4} + x_{n-5}, \quad (n \geq 6), \tag{3.4}$$

and sequences $\{a_n\}, \{b_n\}$ satisfy the equation

$$x_n = 4x_{n-1} - 4x_{n-2} + x_{n-3}, \quad (n \geq 4). \tag{3.5}$$

Proof. According to [13], as

$$\mathbf{M} = \begin{pmatrix} 1 & 1 & 0 & 0 & 0 & 0 & 0 & 0 & 0 & \frac{3}{2} \\ 1 & 2 & 0 & 0 & 0 & 0 & 0 & 0 & 0 & 0 \\ \frac{2}{3} & 0 & 1 & \frac{2}{3} & 0 & 0 & 0 & 0 & 0 & 0 \\ 0 & 1 & \frac{3}{2} & 2 & \frac{5}{6} & 0 & 0 & 0 & 0 & 0 \\ 0 & 0 & \frac{3}{4} & 4 & 6 & 0 & 0 & 0 & 0 & 0 \\ 0 & 0 & \frac{1}{4} & 0 & 0 & 1 & \frac{1}{2} & 0 & 0 & 0 \\ 0 & 0 & 0 & \frac{1}{3} & 0 & 2 & 2 & \frac{5}{3} & 0 & 0 \\ 0 & 0 & 0 & 0 & \frac{1}{2} & 6 & 6 & 6 & 6 & 0 \\ 0 & 0 & 0 & 0 & 0 & 94 & 97 & 101 & 107 & 0 \\ 0 & 0 & 0 & 0 & 0 & 0 & 0 & 0 & 0 & 1 \end{pmatrix} \tag{3.6}$$

is the coefficients matrix of (3.1) with $\text{rank}(\mathbf{M}) = 10$, then the equation from minimal polynomial of matrix \mathbf{M} equals to the characteristic equation of any sequence from (3.1) and s_n . The minimal polynomial of \mathbf{M} is

$$\begin{aligned} p(x) &= x^9 - 128x^8 + 1795x^7 - 8837x^6 + 19239x^5 - 19239x^4 + 8837x^3 - 1795x^2 + 128x - 1 \\ &= (x - 1)(x^2 - 3x + 1)(x^2 - 8x + 1)(x^4 - 116x^3 + 366x^2 - 116x + 1). \end{aligned} \tag{3.7}$$

Thus the recurrences can be describe by (3.3). (The calculation was made by the help of software MAPLE.)

As $a_{n+1}, b_{n+1}, c_{n+1}, d_{n+1}, e_{n+1}$ and v_{n+1} are independent from f_n, g_n, h_n and k_n , they form a system of homogeneous recurrence equations again with matrix $\mathbf{M}_1 = \begin{pmatrix} 1 & 1 & 0 & 0 & 0 & \frac{3}{2} \\ 1 & 2 & 0 & 0 & 0 & 0 \\ \frac{2}{3} & 0 & 1 & \frac{2}{3} & 0 & 0 \\ 0 & 1 & \frac{3}{2} & 2 & \frac{5}{6} & 0 \\ 0 & 0 & \frac{3}{4} & 4 & 6 & 0 \\ 0 & 0 & \frac{1}{4} & 0 & 0 & 1 \\ 0 & 0 & 0 & \frac{1}{3} & 0 & 2 \\ 0 & 0 & 0 & 0 & \frac{1}{2} & 6 \\ 0 & 0 & 0 & 0 & 0 & 94 \\ 0 & 0 & 0 & 0 & 0 & 97 \end{pmatrix}$, where the minimal polynomial is $x^5 - 12x^4 + 37x^3 - 37x^2 + 12x - 1 = (x - 1)(x^2 - 8x + 1)(x^2 - 3x + 1)$. So (3.4) also holds. Similarly, we can reduce the degree of recursion for a_n and b_n . \square

Remark 3.1. In the Euclidean Pascal’s simplex the equation system (3.1) also holds with suitable initial values. In this case, there is no type vertices B, D, E, G, H, K , so $b_i = d_i = e_i = g_i = h_i = k_i = 0$ for any i . Thus the hyperbolic Pascal simplex is not only the geometric but also the algebraic generalization of Pascal’s simplex.

Remark 3.2. The ratios of the numbers of the vertices from level to level tend to the largest eigenvalue of the matrix \mathbf{M} (or dominant root of polynomial (3.7)). According to [6], we can also refer to this limit as the Kepler limit of sequence $\{s_n\}$. Fiorenza and Vincenzi ([6, 7]) gave a necessary and sufficient condition for the existence of Kepler limit. In our case, as all the roots of (7) are different positive real numbers, all the elements of sequence $\{s_n\}$ are also positive, then there exist the Kepler limit and equals to the dominant root. (For more details and examples see [6, 7].) Thus, the growing ratio of \mathcal{HPS} is $\alpha_1 \approx 112.763$, on the contrary it is 1 in the Euclidean case.

4. Sum of the values on levels in hyperbolic Pascal simplex

The sum of the values of the elements on level n in the classical Pascal’s simplex is 4^n ([4]). In this section we determine it in case of the hyperbolic Pascal simplex.

Denote respectively $\hat{a}_n, \hat{b}_n, \hat{c}_n, \hat{d}_n, \hat{e}_n, \hat{f}_n, \hat{g}_n, \hat{h}_n, \hat{k}_n$ and \hat{v}_n , the sums of the values of vertices type $A, B, C, D, E, F, G, H, K$ and 1 on level n , and let \hat{s}_n be the sum of all the values. From Figure 4, 5 and 10 the results of Theorem 4.1 can be read directly. For example, all vertices type A, B and 1 on level i generate, respectively, two, two and three vertices type A on level $i + 1$ and it gives the first equation of (4.1). Table 2 shows the sum of the values of the vertices on levels up to level 10.

Theorem 4.1. *If $n \geq 1$, then*

$$\begin{aligned}
 \hat{a}_{n+1} &= 2\hat{a}_n + 2\hat{b}_n + 3\hat{v}_n, \\
 \hat{b}_{n+1} &= \hat{a}_n + 2\hat{b}_n, \\
 \hat{c}_{n+1} &= 2\hat{a}_n + 3\hat{c}_n + 2\hat{d}_n, \\
 \hat{d}_{n+1} &= 2\hat{b}_n + 3\hat{c}_n + 4\hat{d}_n + 5\hat{e}_n, \\
 \hat{e}_{n+1} &= 3\hat{c}_n + 4\hat{d}_n + 6\hat{e}_n, \\
 \hat{f}_{n+1} &= \hat{c}_n + 4\hat{f}_n + 2\hat{g}_n, \\
 \hat{g}_{n+1} &= \hat{d}_n + 6\hat{f}_n + 6\hat{g}_n + 5\hat{h}_n, \\
 \hat{h}_{n+1} &= \hat{e}_n + 12\hat{f}_n + 12\hat{g}_n + 12\hat{h}_n + 12\hat{k}_n, \\
 \hat{k}_{n+1} &= 94\hat{f}_n + 97\hat{g}_n + 101\hat{h}_n + 107\hat{k}_n \\
 \hat{v}_{n+1} &= \hat{v}_n,
 \end{aligned}
 \tag{4.1}$$

with all zero and $\hat{v}_1 = 4$ initial values.

Table 2. Sum of values of vertices $n \leq 10$

n	0	1	2	3	4	5	6	7	8	9	10
\hat{a}_n	0	0	12	36	108	348	1164	3948	13452	45900	156684
\hat{b}_n	0	0	0	12	60	228	804	2772	9492	32436	110772
\hat{c}_n	0	0	0	24	144	840	5808	48552	458736	4588008	46916592
\hat{d}_n	0	0	0	0	96	1296	14400	152592	1592448	16530384	171272832
\hat{e}_n	0	0	0	0	72	1248	15192	166176	1753080	18264480	189472440
\hat{f}_n	0	0	0	0	24	240	2280	26880	667944	51411168	5797305000
\hat{g}_n	0	0	0	0	0	240	5976	255936	24140328	2793536160	331243298952
\hat{h}_n	0	0	0	0	0	360	38400	4458168	528618816	62831416920	7469847072960
\hat{k}_n	0	0	0	0	0	2256	323592	39296736	4682378232	556809369792	66200381333976
\hat{s}_n	1	4	16	76	508	7060	407620	44411764	5239632532	622525195252	74007676940212

Theorem 4.2. *The sequences $\{\hat{a}_n\}, \dots, \{\hat{k}_n\}$ and $\{\hat{s}_n\}$ can be described by the same tenth order linear homogeneous recurrence sequence*

$$\begin{aligned}
 \hat{x}_n &= 147\hat{x}_{n-1} - 3635\hat{x}_{n-2} + 36277\hat{x}_{n-3} - 175292\hat{x}_{n-4} + 445156\hat{x}_{n-5} - 608920\hat{x}_{n-6} \\
 &\quad + 438532\hat{x}_{n-7} - 151320\hat{x}_{n-8} + 19344\hat{x}_{n-9} - 288\hat{x}_{n-10}, \quad (n \geq 11), \tag{4.2}
 \end{aligned}$$

the initial values are in Table 2. The sequences $\{\hat{a}_n\}, \dots, \{\hat{e}_n\}$ can also be described by

$$\hat{x}_n = 18\hat{x}_{n-1} - 99\hat{x}_{n-2} + 226\hat{x}_{n-3} - 224\hat{x}_{n-4} + 92\hat{x}_{n-5} - 12\hat{x}_{n-6}, \quad (n \geq 7), \tag{4.3}$$

and sequences $\{\hat{a}_n\}, \{\hat{b}_n\}$ can also be formed by

$$\hat{x}_n = 5\hat{x}_{n-1} - 6\hat{x}_{n-2} + 2\hat{x}_{n-3}, \quad (n \geq 4). \tag{4.4}$$

The proof of this theorem is the same step by step as the proof of Theorem 3.2. The factorised minimal polynomial (now it is the same as the characteristic polynomial) of the coefficients matrix of (4.1) is

$$\begin{aligned}
 p(x) &= x^{10} - 147x^9 + 3635x^8 - 36277x^7 + 175292x^6 - 445156x^5 \\
 &\quad + 608920x^4 - 438532x^3 + 151320x^2 - 19344x + 288 \\
 &= (x - 1)(x^2 - 4x + 2)(x^3 - 13x^2 + 28x - 6)(x^4 - 129x^3 + 1214x^2 - 1428x + 24).
 \end{aligned}
 \tag{4.5}$$

Remark 4.1. The growing ratio (or Kepler limit) of values of *HPS* is ≈ 118.89 (conditions hold, see Remark 3.2 and [6, 7]), while it is 4 in Euclidean case.

References

- [1] Anatriello, G. and Vincenzi, G., Tribonacci-like sequences and generalized Pascal's pyramids. *Internat. J. Math. Ed. Sci. Tech.*, **45** (2014), 1220-1232.
- [2] Belbachir, H., Németh, L. and Szalay, L., Hyperbolic Pascal triangles. *Appl. Math. Comp.*, **273** (2016), 453-464.
- [3] Belbachir, H. and Szalay, L., On the arithmetic triangles. *Šiauliai Math. Sem.*, **9** (2014), 15-26.
- [4] Bondarenko, B. A., Generalized Pascal triangles and pyramids, their fractals, graphs, and applications. Translated from the Russian by Bollinger, R. C. (English) Santa Clara, CA: The Fibonacci Association, vii, 253 p. 1993. www.fq.math.ca/pascal.html
- [5] Coxeter, H. S. M., Regular honeycombs in hyperbolic space. *Proc. Int. Congress Math.*, Amsterdam, **Vol. III.** (1954), 155-169.
- [6] Fiorenza, A. and Vincenzi, G., Limit of ratio of consecutive terms for general order-k linear homogeneous recurrences with constant coefficients. *Chaos, Solitons & Fractals*, **44** (2011), 147-152.
- [7] Fiorenza, A. and Vincenzi, G., From Fibonacci Sequence to the Golden Ratio. *Journal of Mathematics*, (2013), Article ID 204674, 3 pages.
- [8] Harris, J. M., Hirst, J. L. and Mossinghoff, M. J., *Combinatorics and Graph Theory*. Springer, 2008.
- [9] Németh, L. and Szalay, L., Alternating sums in hyperbolic Pascal triangles. *Miskolc Mathematical Notes*, **17** (2016), no. 2, 989-998.
- [10] Németh, L. – Szalay, L., Recurrence sequences in the hyperbolic Pascal triangle corresponding to the regular mosaic $\{4, 5\}$. *Annales Mathematicae et Informaticae*, **46** (2016), 165–173.
- [11] Németh, L. and Szalay, L., Power sums in hyperbolic Pascal triangles. *Analele Univ. "Ovidius", Math Series.*, (2018) (to appear).
- [12] Németh, L., Fibonacci words in hyperbolic Pascal triangles. *Acta Universitatis Sapientiae Mathematica*, **9** (2017) no. 2, (to appear).
- [13] Németh, L., On the hyperbolic Pascal pyramid. *Beitr Algebra Geom.*, **57** (2016), 913–927.
- [14] Németh, L., On the 4-dimensional hypercube mosaics. *Publ. Math. Debrecen*, **70** (2007), no. 3–4, 291–305.
- [15] Németh, L., Pascal pyramid in space $\mathbf{H}^2 \times \mathbf{R}$. *Mathematical Communications*, **22** (2017), 211-225.
- [16] Németh, L., The growing ration of hyperbolic regular mosaics with bounded cell, *Armenian Journal of Mathematics*, **9** (2017), 1-19.
- [17] Siani, S. and Vincenzi, G., Fibonacci-like sequences and generalized Pascal's triangles. *Internat. J. Math. Ed. Sci. Tech.*, **45** (2014), 609-614.

Affiliations

LÁSZLÓ NÉMETH

ADDRESS: University of Sopron, Institute of Mathematics, 9400, Sopron - Hungary

E-MAIL: nemeth.laszlo@uni-sopron.hu

ORCID ID : orcid.org/0000-0001-9062-9280